Available online at www.sciencedirect.com
SCIENCE DIRECT®
Analytica Chimica Acta 504 (2004) 101–111
ANALYTICA CHIMICA ACTA
www.elsevier.com/locate/aca

Analysis of NAD(P)$^+$ and NAD(P)H cofactors by means of imprinted polymers associated with Au surfaces: A surface plasmon resonance study

Oleg A. Raitman, Vladimir I. Chegel[1], Andrei B. Kharitonov*, Maya Zayats, Eugenii Katz, Itamar Willner

Department of Organic Chemistry, Institute of Chemistry, The Hebrew University of Jerusalem, Jerusalem 91904, Israel

Received 6 January 2003; received in revised form 14 April 2003; accepted 23 April 2003

Abstract

Crosslinked films consisting of the acrylamide-acrylamidophenylboronic acid copolymer that are imprinted with recognition sites for β-nicotinamide adenine dinucleotide (NAD$^+$), β-nicotinamide adenine dinucleotide phosphate NADP$^+$, and their reduced forms (NAD(P)H), are assembled on Au-coated glass supports. The binding of the oxidized cofactors NAD$^+$ or NADP$^+$ or the reduced cofactors NADH or NADPH to the respective imprinted sites results in the swelling of the polymer films through the uptake of water. Surface plasmon resonance (SPR) spectroscopy is employed to follow the binding of the different cofactors to the respective imprinted sites. The imprinted recognition sites reveal selectivity towards the association of the imprinted cofactors. The method enables the analysis of the NAD(P)$^+$ and NAD(P)H cofactors in the concentration range of 1×10^{-6} to 1×10^{-3} M. The cofactor-imprinted films associated with the Au-coated glass supports act as active interfaces for the characterization of biocatalyzed transformations that involve the cofactor-dependent enzymes. This is exemplified with the characterization of the biocatalyzed oxidation of lactate to pyruvate in the presence of NAD$^+$ and lactate dehydrogenase using the NADH-imprinted polymer film.

Keywords: Surface plasmon resonance; NAD(P)$^+$ and NAD(P)H cofactors; Imprinted polymers; Sensor

1. Introduction

The quantitative analysis of the oxidized cofactors β-nicotinamide adenine dinucleotide (NAD$^+$), and β-nicotinamide adenine dinucleotide phosphate NADP$^+$, and the respective reduced cofactors (NAD(P)H), are of importance in developing biosensors involving NAD(P)$^+$/NAD(P)H-dependent enzymes [1], and in the monitoring of biocatalyzed transformations that involve NAD(P)$^+$/NAD(P)H-dependent enzymes [2]. The amperometric analysis of NAD(P)$^+$ reveals irreversible electrochemical reduction accompanied by high overpotentials [3] resulting in a non-enzymatically-active dimer [4]. The NAD(P)$^+$ cofactors were reduced electrocatalytically or bioelectrocatalytically in the presence of Rh-complexes [5], or in the presence of NAD(P)$^+$-dependent enzymes e.g. ferredoxin-NADP$^+$ reductase, lipoamide dehydrogenase, formate dehydrogenase) [6]. Direct, non-mediated electrochemical reduction of NAD(P)$^+$ was also achieved at modified electrodes, e.g. in the presence of a L-histidine-modified Ag-electrode [7]. Similarly, the direct oxidation of NAD(P)H is electrochemically irreversible and involves high overpotentials [8]. The electrocatalyzed two-electron oxidation of NAD(P)H was extensively studied in the presence of different electrocatalysts [9], for example *o*-quinones [10], phenazine, phenoxazine and phenothiazine derivatives [11]. There is no method, however, to selectively analyze NAD$^+$ in the presence of NADP$^+$ or alternatively to selectively analyze NADH and NADPH.

Imprinting of molecular recognition sites in organic [12] or inorganic polymers [13,14] has been the subject of extensive research efforts. There are two general methods to generate imprinted sites in polymer membranes. One approach

* Corresponding author. Tel.: +972-2-6585272; fax: +972-2-6527715.
E-mail address: willnea@vms.huji.ac.il (A.B. Kharitonov).
[1] On leave from the Institute of Physics of Semiconductors, National Academy of Sciences of Ukraine, Kiev, Ukraine.

0003-2670/$ – see front matter © 2003 Elsevier B.V. All rights reserved.
doi:10.1016/S0003-2670(03)00511-7

[15] involves the polymerization of monomers that include a complementary function to the imprinted substrate such as H-bonds, electrostatic interactions, and π-donor–acceptor interactions. Polymerization of the monomer–substrate complex, followed by the removal of the substrate molecules acting as a template for the polymerization, yields the imprinted sites in the polymer. The second approach involves the covalent attachment [16] or coordination [17] of the substrate to polymerizable monomer units, followed by the copolymerization of the functional monomers with other monomers, to yield rigidified polymer matrices. Cleavage of the polymer-linked substrate units leads to the formation of the polymer with imprinted sites. The advantages of both covalent and non-covalent imprinting methods can also be combined to generate molecularly imprinted recognition sites in polymeric films as reported by Whitcombe et al. [18]. Polymers with imprinted sites revealing structural [19] and chiral [20,21] selectivities, have been prepared. The imprinted polymers have been used as specific sensing interfaces [22], functional materials for chromatographic separations [23] and matrices for selective and catalyzed chemical transformations [24]. The use of imprinted polymers is particularly tempting for sensing applications since membranes with tailored recognition functions can be generated. The major difficulty encountered in the use of imprinted polymers as active components in sensor devices is, however, the coupling of the sensing membrane with an electronic transducer. The imprinted organic polymer is usually relatively thick, and the recognition sites lack direct electrical contact with the transducer. Indeed, most of the sensor devices based on imprinted polymers are either optical, and include chromogenic markers [25], or involve the microgravimetric analysis of the bound substrate using piezoelectric crystals (quartz crystal microbalance (QCM)) [26].

Boronic acid ligands bind strongly and reversibly vicinal diols (Eq. (1)). This property has been employed to develop optical sensors for sugars [27] or gelating materials [28] that undergo sol–gel transitions upon the binding of the sugar. Boronic acid acrylamide copolymers were employed as active matrices for the sensing of glucose [29] or nucleotides [30]. The boronic acid ligand is often used to imprint molecular recognition sites in polymers for specific binding [31] and separation [32] of sugars.

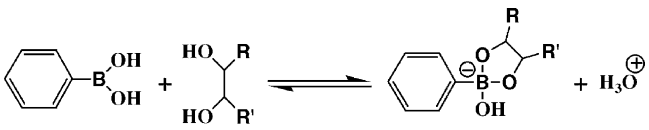

(1)

Recently, we reported on the selective analysis of the NAD^+, $NADP^+$, NADH and NADPH cofactors in acrylamide-acrylamidophenylboronic acid copolymer membranes associated with ISFET devices, and we applied the functional devices to follow biocatalyzed transformations [30]. In complementary microgravimetric quartz crystal microbalance experiments, we found that the association of the $NAD(P)^+$ or the NAD(P)H cofactors to the imprinted polymer matrices linked to the Au-quartz crystals involved the uptake of water and the swelling of the polymer films [30]. Surface plasmon resonance (SPR) spectroscopy is a versatile tool to characterize the optical and structural features of thin films associated with metallic, e.g. Au or Ag surfaces [33]. The pattern of the SPR spectrum is controlled by the refractive index of the film medium and the thickness of the film associated with the metal interface. Indeed, SPR spectroscopy was extensively used to characterize polymer films on surfaces [34], to follow redox-transformations in polymers [35], to characterize biorecognition processes such as antigen-antibody [36] or nucleic acid–DNA interactions [37], and to follow bioelectrocatalytic transformations [34,38]. Here we report on the analysis of $NAD(P)^+$ and NAD(P)H cofactors by means of an imprinted polymer film, using SPR spectroscopy. We demonstrate the use of the functional interface to follow a bioelcatalyzed transformation that includes the NAD^+-dependent enzyme lactate dehydrogenase. Only a few reports have addressed the use of SPR to follow the association of substrates to imprinted polymers [39–41]. In these studies, however, the SPR spectra followed mass changes associated with the binding of the substrate to the polymer. These mass changes (for low molecular-weight substrates) are small, resulting in low signals and limited analytical performance of the respective sensors. In the present work, we apply imprinted polymers that undergo a swelling process upon binding of the substrates, resulting in a substantial change in the refractive index of the polymer sensing interface. This enables the improved application of SPR spectroscopy to follow the association of substrates to the imprinted polymers.

2. Experimental

2.1. Materials

The acrylic acid monomer functionalized with 3-amino phenylboronic acid, acrylamidophenylboronic acid, was synthesized according to the published procedure [42].

Acrylamide, *N*,*N*′-methylene-bisacrylamide, *N*,*N*,*N*′,*N*′-tetramethylethylenediamine, ammonium persulfate acrylic acid, sodium salts of β-NAD^+, β-NADH, β-$NADP^+$, β-NADH, as well as L(+)-lactic acid and the enzyme lactate dehydrogenase (LDH, E.C. 1.1.1.27 from rabbit muscle, type XI) were purchased from Sigma or Aldrich, and cystamine from Fluka. Ultrapure water from Serapur PRO90CN was used throughout the experiments.

2.2. Preparation of the polymer-modified surfaces

The glass supports (TF-1 glass, 20 mm × 20 mm) covered with a Cr sublayer (∼5 nm) and a polycrystalline Au layer (∼50 nm) (Analytical-μSystem, Ger-

many) were preliminarily functionalized with cystamine (50 mM solution in phosphate buffer, pH = 7.3, for 3 h). Then the slides were rinsed with distilled water, and reacted with a solution containing 1×10^{-2} M acrylic acid in HEPES buffer, pH = 7.4, in the presence of 1-[3-(dimethylamino)propyl]-3-ethylcarbodiimide hydrochloride (EDC) (10 mM) for 2 h. After these modifications, the slides were washed with distilled water and flushed by a flow of nitrogen. For the preparation of the imprinted polymeric membrane and its coupling to the prefunctinalized surface of SPR Au-covered glass plates, the slides were immersed into a mixture composed of acrylamide (0.5 M), 3-acrylamidophenylboronic acid (0.01 M) as functional monomers, *N*,*N*′-methylenebisacrylamide (0.2 M) as a crosslinker, and the respective template substrates (NAD^+, $NADP^+$, NADH or NADPH) for 1 h, and then a drop of the mixture consisting of ammonium persulfate (0.02 M) and *N*,*N*,*N*′,*N*′-tetramethylenediamine (10% (v/v)) as initiators was spread over the plate. The resulting modified surfaces were allowed to dry in air overnight. To eliminate the imprinted template molecules, the modified surfaces were thoroughly rinsed with 1% NH_3 solution, and further rinsed with phosphate buffer, pH = 7.3 and water, until stable SPR response was obtained. The resulting surfaces were then used for the respective analyses.

2.3. Measurements and treatment of the results

The SPR Kretschmann-type spectrometer Biosuplar-2 (Analytical-μSystem; light-emitting diode light source, λ = 670 nm) was used in this work. A high refraction index of the prism ($n = 1.61$) and a broad dynamic range (up to 19° in air) of the SPR instrument enabled the SPR analyses of relatively thick polymeric films (up to 200 nm) without change of the initial angle. This is an important condition for the quality of the computer fitting of the experimental data with a theoretical curve. The SPR data were processed using Biosuplar-2 software (2.2.30). The experimental SPR spectra of the polymeric film were fitted to the theoretical curves on the basis of five-phase Fresnel calculations using the Nelder–Mead algorithm of minimization [43].

The SPR sensograms represent real time changes in the minimum reflectivity angle and are recorded using a home-built flow cell.

The accuracy of the measurements was ±5% for five independent measurements. The plates reproducibility was found to be about 15% for five various plates.

3. Results and discussion

Each of the oxidized cofactors NAD^+ or $NADP^+$, and the reduced cofactors NADH or NADPH (Fig. 1), were imprinted in a crosslinked acrylamide-acrylamidophenylboronic acid copolymer associated with an Au-coated glass support. The method for the generation of the imprinted polymer is schematically depicted in Fig. 2. As the $NAD(P)^+$ or NAD(P)H cofactors include ribose units, the cofactors yield a complex with the 3-acrylamidophenylboronic acid. This linkage, together with complementary H-bonds between the

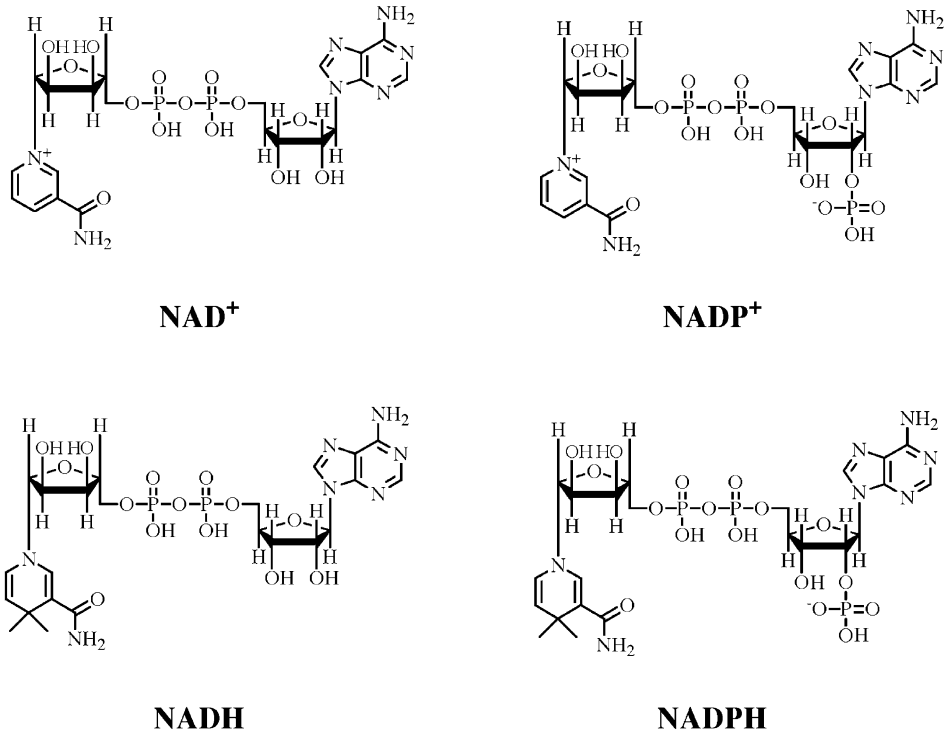

Fig. 1. Structures of $NAD(P)^+$ and NAD(P)H cofactors.

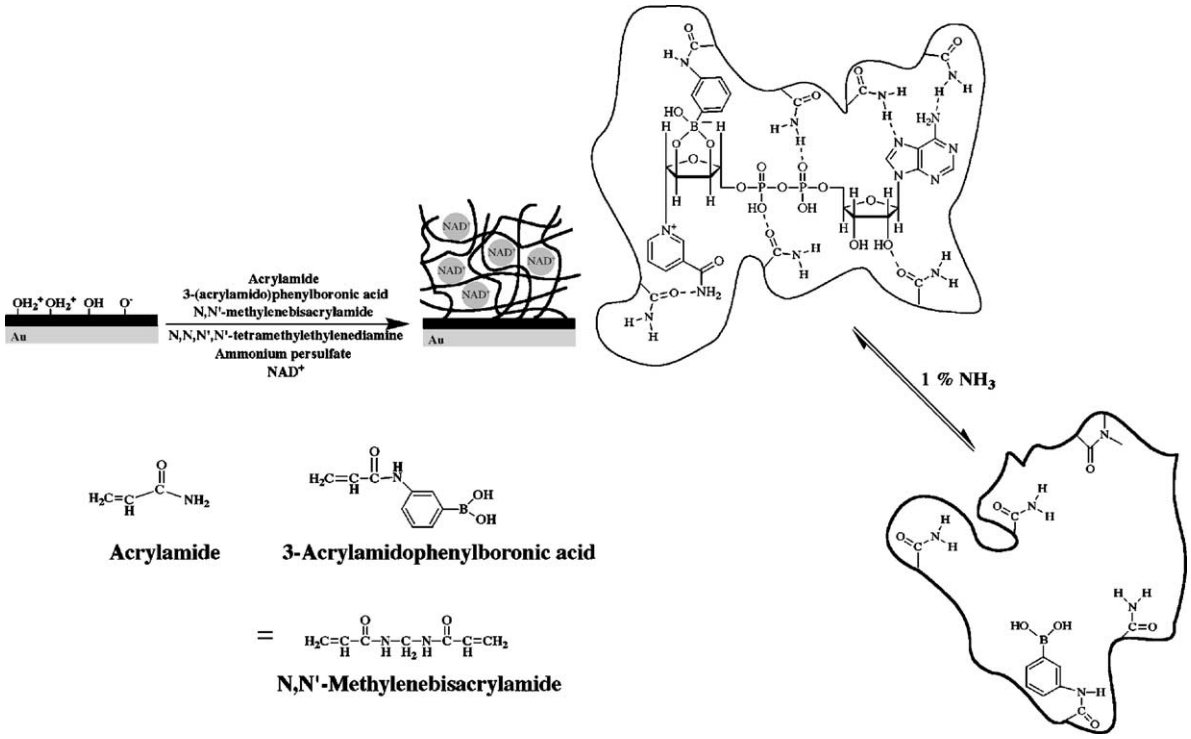

Fig. 2. Schematic preparation of the $NAD(P)^+$/NAD(P)H cofactors-imprinted acrylamide-acrylamidophenylboronic acid copolymer sensing film on an Au-coated glass support. The support was primarily modified with cystamine monolayer followed by its coupling to acrylic acid. The scheme exemplifies the imprinting of NAD^+.

different functional units of the cofactors and the acrylamide and 3-acrylamidophenylboronic acid monomers, lead, upon polymerization accompanied by crosslinking in the presence of *N*,*N*′-methylene bisacrylamide, to the cofactor-embedded polymer matrices. To improve the adhesion of the imprinted polymer film on the Au-coated glass support, a primary cystamine monolayer is assembled on the Au-surface, and acrylic acid is covalently linked to the monolayer interface. Thus, upon the radical-induced polymerization of the film, the solution-solubilized monomers are copolymerized with the surface-confined monomer units, leading to a surface-bound crosslinked film. The elimination of the template cofactors with 1% NH_3 generates the imprinted sites for the respective cofactors. The existence of functional groups at the periphery of the imprinted molecular contours (boronic acid residues, amide-functionalities, etc.) is expected to yield selective sites for the accommodation of the respective oxidized or reduced cofactors.

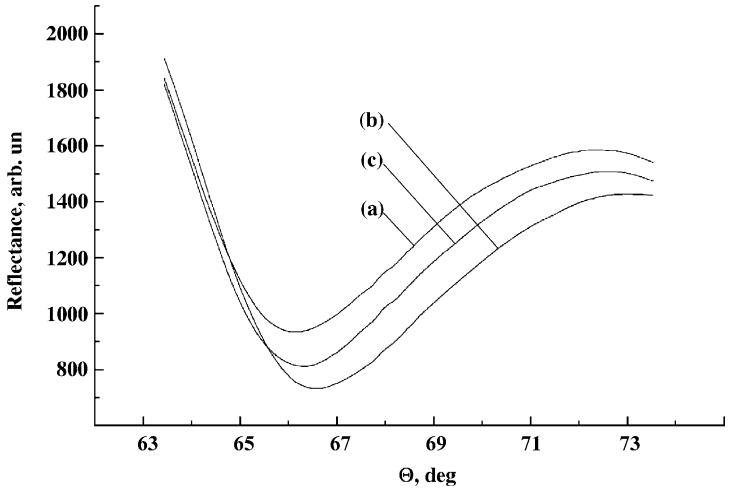

Fig. 3. The SPR spectra of (a) the bare Au-coated glass support; (b) and (c) the Au electrode after the assembly of the NAD^+-imprinted acrylamide-acrylamidophenylboronic acid copolymer with and without the template molecules, respectively.

Fig. 3 shows the SPR spectra of the bare Au-surface, curve (a), after the assembly of the NAD^+-imprinted polymer film, curve (b), and after rinsing of the NAD^+-imprinted film with 1% NH_3 solution, curve (c). By fitting of the five independent SPR spectra of the film-modified surface, the calculated film thickness corresponds to 22 ± 3 nm. The shift in the minimum reflectivity angle observed, before (curve b) and after the imprinted polymer rinsing (curve c), corresponds to the elimination of the imprinted NAD^+ from the polymer. Using Eq. (2) where Γ is the surface coverage, d the thickness of the assembled layer, n_1 and n_2 correspond to refractive indexes of media near the electrode surface before and after a recognition event, the term (dn/dc) reflects the influence of the analyte concentration on the refractive index of the surrounding medium which in this case corresponds to $0.188\,cm^3\,g^{-1}$, the fitted values of the refractive index of the polymer (n_1 and n_2) before and after the washing procedure ($n_1 = 1.45$ and $n_2 = 1.40$, respectively), we estimated the loading of the imprinted NAD^+ sites in the polymer to be $22.6\,ng\,mm^{-2}$.

$$\Gamma = \frac{d(n_1 - n_2)}{dn/dc} \quad (2)$$

Fig. 4(A) shows the SPR spectra of the NAD^+-imprinted polymer film in the absence of NAD^+, curve (a), and after treatment with NAD^+, 1×10^{-3} M, curve (b). The minimum reflectivity angle is shifted to lower values. In a control experiment, an acrylamide-acrylamidophenylboronic acid copolymer film was assembled on the Au-surface without the imprint of the NAD^+ cofactor. Treatment of the non-imprinted film with NAD^+, 1×10^{-3} M, does not yield any noticeable change in the SPR spectrum of the film. This control experiment clearly indicates that no non-specific binding of NAD^+ to the polymer takes place. It also reveals that minute changes in the refractive index of the solution resulting upon solubilization of NAD^+, do not affect the SPR spectrum. Thus, the changes in the SPR spectrum upon interaction with NAD^+ originate from the specific association of the oxidized cofactor to the imprinted sites. The SPR spectrum shown in curve (b) was fitted to the theoretical curves on the basis of five-phase Fresnel calculations using the Nelder–Mead algorithm of minimization [43]. The fitting indicates a decrease in the refractive index of the polymer upon the association of NAD^+ ($n_1 = 1.45$ and $n_2 = 1.40$ before and after the association of NAD^+, respectively) and an increase in the polymer thickness of 3.0 ± 0.2 nm, as a result of the swelling of the polymer film. The changes in the SPR-spectrum of the NAD^+-imprinted polymer film are controlled by the bulk concentration of NAD^+ in solution. Also, the NAD^+-imprinted polymer film reveals selectivity upon analysis of the imprinted cofactor. Fig. 4(B) shows the sensogram corresponding to the changes in the minimum reflectivity angles of the SPR spectra in the course of analyzing different concentrations of the different oxidized and reduced cofactors by the NAD^+-imprinted film. In this experiment, the NAD^+-imprinted film is initially treated with different concentrations of NAD^+. Clearly, as the bulk concentration of NAD^+ increases, the minimum reflectivity angle decreases, and bulk concentrations of NAD^+ as low as 1×10^{-6} M can be sensed by the system. The swelling of the polymer should increase the mass associated with the sensing interface, as a result of the uptake of water, and concomitantly, should decrease the refractive index of the sensing medium. The increase in mass of the polymer should be reflected by an increase in the minimum reflectivity angle of the SPR spectrum, whereas the decrease in the refractive index of the film should lower the minimum reflectivity angle of the polymer interface. Experimentally, we observe that the swelling of the polymer upon the binding of NAD^+ to the imprinted sites results in a decrease in the minimum reflectivity angle, implying that the changes in the refractive index of the polymer, as a result of the swelling, contribute mostly to the overall features of the experimental SPR spectra. After the completion of the analysis cycle of NAD^+, the film is washed with water. The bound NAD^+ is washed off as evident by the fact that the original minimum reflectivity angle of the imprinted film that lacks bound NAD^+ is achieved. The resulting film was then interacted with the NADH cofactor using different concentrations (1×10^{-6} to 1×10^{-3} M). Only minute changes in the minimum reflectivity angle are observed. Similarly, washing off the bound NADH and treatment of the NAD^+-imprinted film with $NADP^+$ or NADPH, respectively, do not yield any changes in the minimum reflectivity angles of the SPR spectra of the film. To reveal that the NAD^+-imprinted film remained functionally intact towards the sensing of NAD^+, the system that was employed for the analysis of NAD^+, NADH, $NADP^+$ and NADPH was applied again for the analysis of variable concentrations of NAD^+. Clearly, the changes in the minimum reflectivity angle of the SPR spectra characteristic to the film in the presence of variable bulk concentrations of NAD^+ are reproduced, similarly to the first analysis cycle of NAD^+. These experiments clearly indicate that the NAD^+-imprinted polymer film reveals selectivity towards the imprinted substrate, and that the oxidized cofactor $NADP^+$ or the reduced cofactors NADH or NADPH exhibit low affinity, or no affinity, for the imprinted sites. Fig. 4(C) depicts the calibration curves corresponding to the changes in the minimum reflectivity angles of the NAD^+-imprinted film upon the analysis of the different cofactors. The NAD^+-imprinted film revealed stability for at least 10 days upon daily operation (with only 10% decay in the outcome signal but with no lack in the selectivity).

Fig. 5(A) shows the SPR spectra of the $NADP^+$-imprinted polymer film before the interaction with $NADP^+$, curve (a) and after treatment with $NADP^+$, 1×10^{-3} M curve (b). As before, binding of $NADP^+$ to the imprinted polymer results in a shift in the minimum reflectivity angle. Theoretical fitting of the SPR spectrum after the association of $NADP^+$ indicates a decrease in the refractive index of the

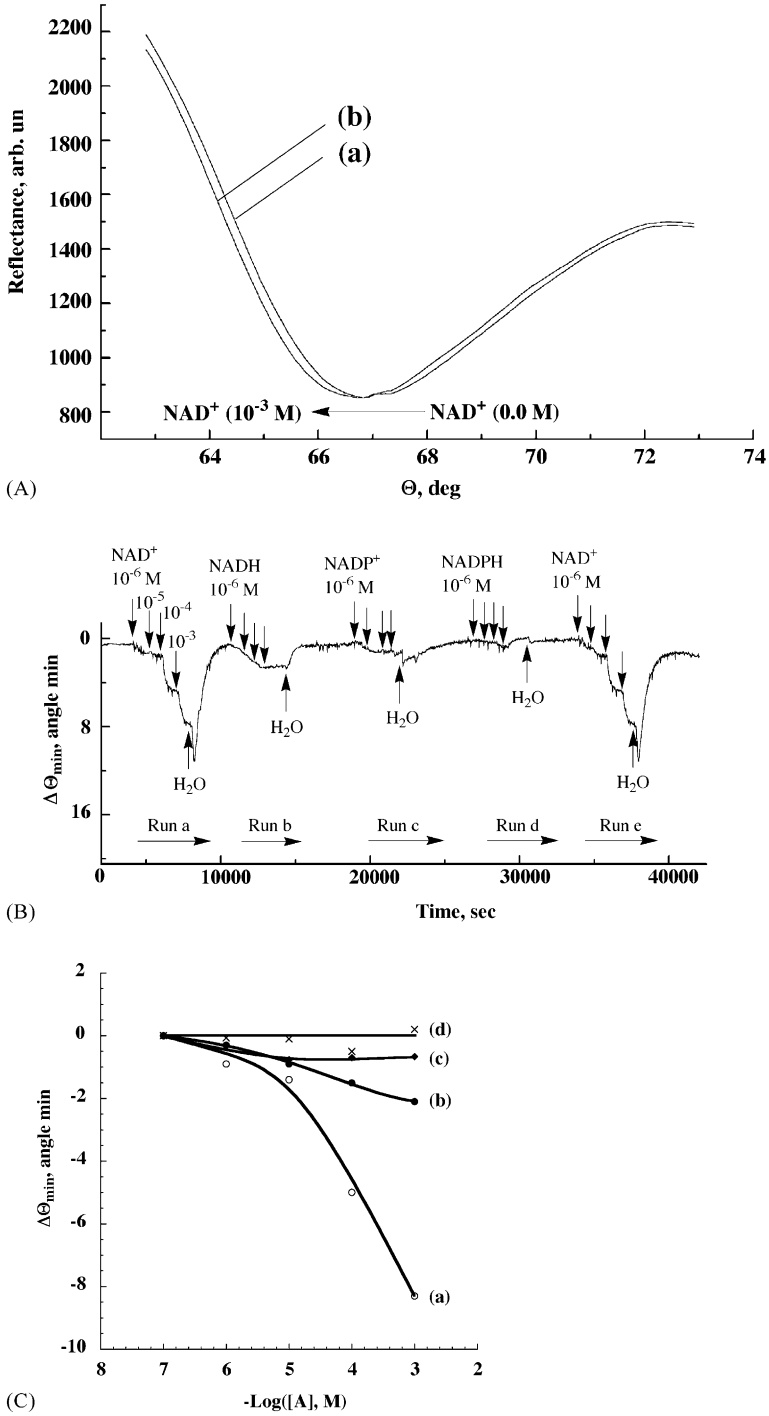

Fig. 4. (A) The SPR spectra of the gold-coated glass modified with the NAD^+-imprinted acrylamide-acrylamidophenylboronic acid copolymer recorded: (a) after the removal of the NAD^+ template molecules; and (b) after its treatment with NAD^+ (1×10^{-3} M) solution. (B) The SPR sensogram corresponding to the analyses of 1×10^{-7} to 1×10^{-3} solutions of: (a) NAD^+, (b) NADH, (c) $NADP^+$, and (d) NADPH by the NAD^+-imprinted polymer film. Run (e) corresponds to repetitive analyses of NAD^+ by the imprinted film. The numbers correspond to the respective analyte concentrations. (C) Calibration plots corresponding to the changes in the minimum reflectivity angles at variable concentrations of the $NAD(P)^+$/NAD(P)H cofactors: (a) for NAD^+, (b) for NADH, (c) for $NADP^+$ and (d) for NADPH.

polymer from $n_1 = 1.45$ to $n_2 = 1.40$ and an increase in the film thickness of ca. 5.0 ± 0.3 nm as a result of binding of $NADP^+$. This increase in the polymer thickness is attributed to the swelling of the film that accompanies the binding of the substrate. Control experiments reveal that $NADP^+$ does not yield any change in the SPR spectrum of a non-imprinted acrylamide-acrylamidophenylboronic acid copolymer film, implying that no non-specific binding of $NADP^+$ to the polymer film occurs. Fig. 5(B) shows the sensogram corresponding to the observed changes of

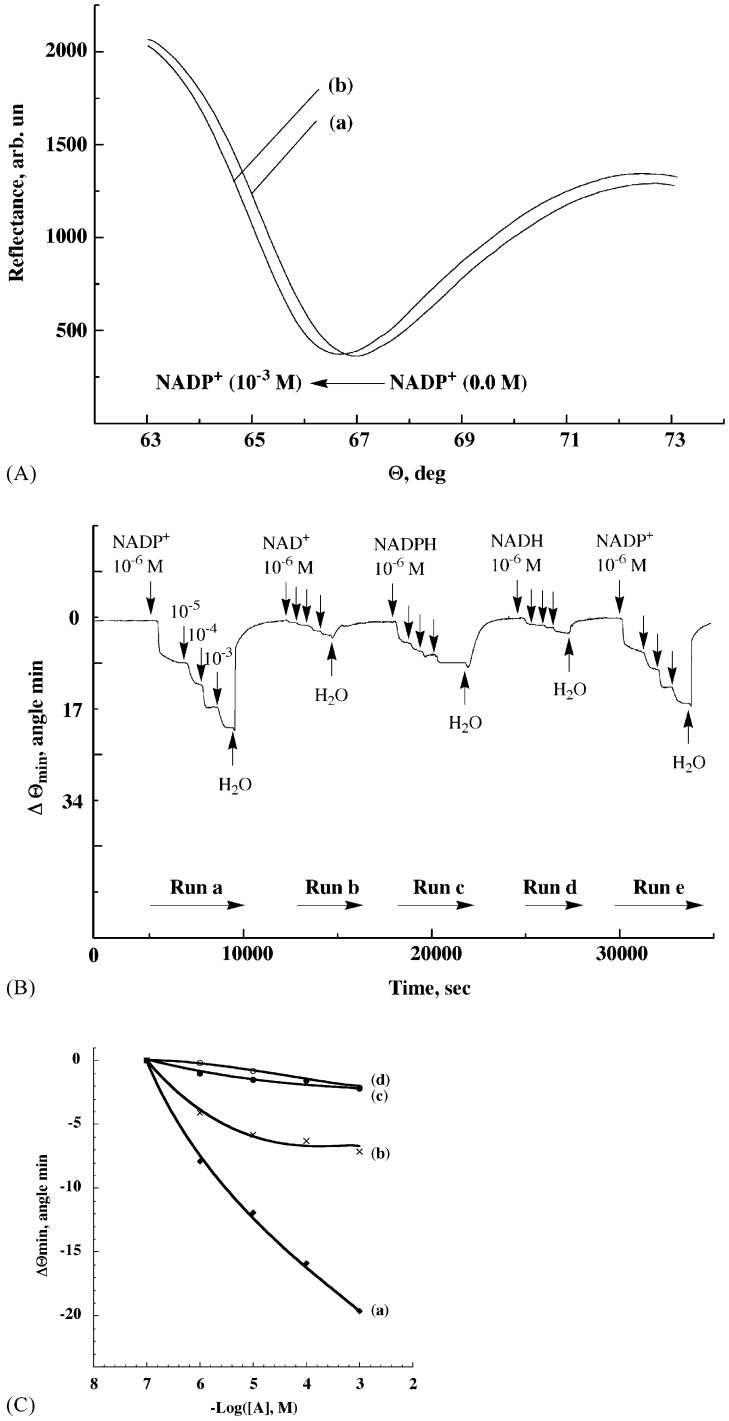

Fig. 5. (A) The SPR spectra of the gold coated glass modified with the $NADP^+$-imprinted acrylamide-acrylamidophenylboronic acid copolymer recorded: (a) after the removal of the $NADP^+$ template molecules, and (b) after the treatment with 1×10^{-3} M $NADP^+$ solution. (B) The SPR sensogram corresponding to the analyses of 1×10^{-7} to 1×10^{-3} M solutions of: (a) $NADP^+$, (b) NAD^+, (c) NADPH and (d) NADH by the $NADP^+$-imprinted polymeric film. Run (e) corresponds to repetitive analysis of $NADP^+$. The numbers correspond to the respective analyte concentrations. (C) Calibration plots corresponding to the changes in the minimum reflectivity angles at variable concentrations of the $NAD(P)^+$/NAD(P)H cofactors: (a) for $NADP^+$, (b) for NADPH, (c) for NAD^+ and (d) for NADH.

the minimum reflectivity angles of the $NADP^+$-imprinted polymer upon interaction with different concentrations of $NADP^+$ (1×10^{-6} to 1×10^{-3} M) (Fig. 5(B), run (a)). As the concentration of $NADP^+$ increases, the shift in the minimum reflectivity angle is enhanced. Fig. 5(B), runs (b), (c) and (d) show the changes in the minimum reflectivity angles of the $NADP^+$-imprinted film upon analyzing the non-imprinted cofactors NAD^+, NADPH and NADH, respectively. Minute changes in the minimum reflectivity angles of the film are observed in the presence of NAD^+

and NADH, indicating that these two cofactors exhibit very little affinity to the $NADP^+$-imprinted sites. For the reduced cofactor NADPH we observe some decrease in the minimum reflectivity angles upon interaction with the $NADP^+$-imprinted polymer. This result is very similar to that observed for the NAD^+-imprinted polymer, where some affinity towards NADH was also observed. This may be explained by the fact that the molecular contours for NAD^+ and $NADP^+$ reveal some affinity for the respective reduced cofactors. Alternatively, the reduced cofactors NADH or NADPH always include, as impurities, the oxidized cofactors NAD^+ and $NADP^+$, and thus the observed responses may originate from these components. It is interesting to note that the NAD^+-imprinted polymer is unaffected in the presence of $NADP^+$, and the $NADP^+$-imprinted film is not affected by the NAD^+ cofactors. Thus, the imprinting procedure leads to impressive selectivity where the single phosphate substituent differentiating $NADP^+$ from NAD^+ is sufficient to generate specific molecular contours for the respective cofactors. The $NADP^+$ imprinted film is still functionally active to analyze $NADP^+$ after the completion of the NAD^+, NADPH and NADH detection cycle. Fig. 5(B), run (e) shows the re-analysis of the $NADP^+$ cofactor by the functionalized film. The sensor reveals cyclic selective activity for analyzing $NADP^+$ for at least 10 days upon daily operation with ca. 12% decay in the SPR signal. It should be noted that within the time interval of 10 days, the film thickness remained unaltered, suggesting that the slight degradation in the performance of the imprinted interface originates from the structural perturbation of the imprinted sites. Fig. 5(C) shows the calibration curve that corresponds to the changes in the minimum

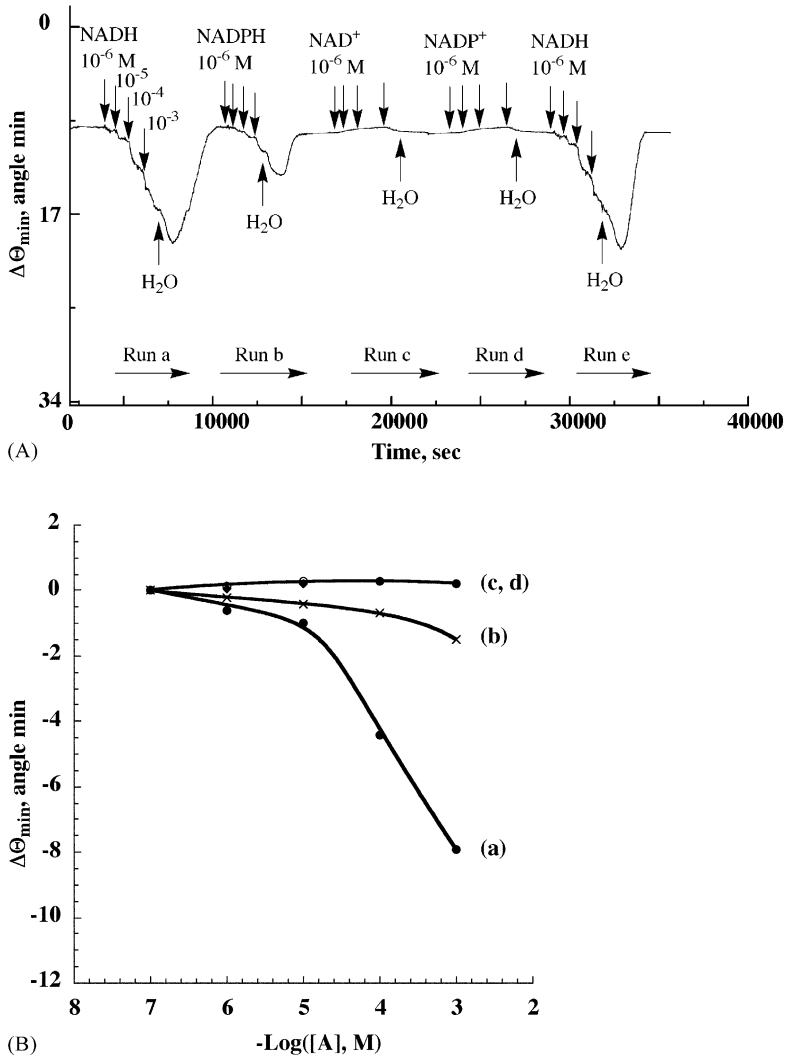

Fig. 6. (A) The SPR sensogram corresponding to the analyses of 1×10^{-7} to 1×10^{-3} M solutions of (a) NADH, (b) NADPH, (c) NAD^+, and (d) $NADP^+$ by the NADH-imprinted polymeric film. Run (e) corresponds to repetitive analysis of NADH. The numbers correspond to the respective analyte concentrations. (B) Calibration plots corresponding to the changes in the minimum reflectivity angles at variable concentrations of the $NAD(P)^+$/NAD(P)H cofactors: (a) for NADH, (b) for NADPH, (c) for NAD^+ and (d) for $NADP^+$.

reflectivity angles upon analyzing $NADP^+$ by the $NADP^+$-imprinted polymer. For comparison, the changes in the minimum reflectivity angles of the $NADP^+$ imprinted film upon interaction with the other cofactors are also shown.

Related results are observed upon imprinting of the reduced cofactors NADH or NADPH in the crosslinked acrylamide-acrylamidophenylboronic acid copolymer. Fig. 6(A) shows the sensogram corresponding to the changes of the minimum reflectivity angles of the NADH-imprinted polymer upon interaction with various concentrations of NADH (1×10^{-6} to 1×10^{-3} M), run (a), and as a result of the treatment of the NADH-imprinted polymer with NADPH, NAD^+ and $NADP^+$, runs (b), (c) and (d), respectively. After completion of the analysis cycles of NADPH, NAD^+ and NADH, the sensing activity of the imprinted polymer towards NADH is regenerated (Fig. 6(A), run (e)). Fig. 6(B) shows the calibration curves that correspond to the changes in the minimum reflectivity angles of the NADH-imprinted film upon analyzing variable concentrations of NADH, and upon treatment with variable concentrations of the other cofactors.

Fig. 7(A) shows the sensogram that corresponds to the analysis of different concentrations of NAD(P)H by the NADPH-imprinted membrane, run (a), and the responses of the NADPH-imprinted polymer to different concentrations of the other cofactors, NADH, NAD^+ and $NADP^+$, runs (b), (c) and (d), respectively. The ability of the NADPH-imprinted polymer to regenerate its function towards the sensing of NADPH is depicted in Fig. 7(A), run (e). Fig. 7(B) shows the calibration curves corresponding to the changes in the minimum reflectivity angles of the NADPH-imprinted polymer upon analyzing NADPH and

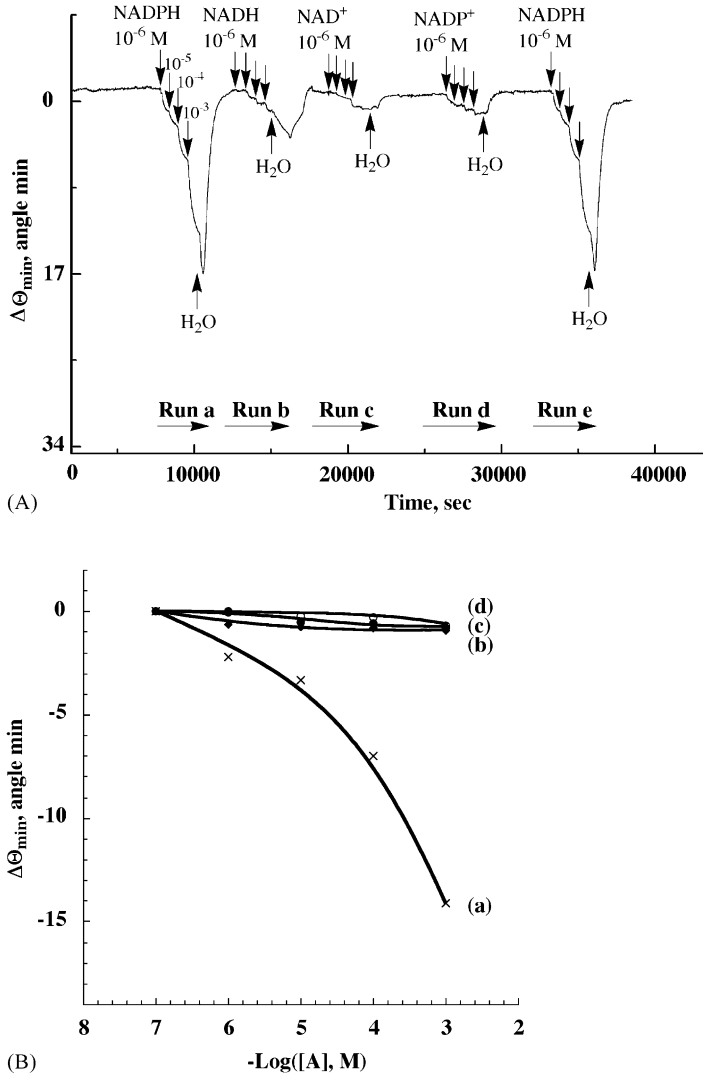

Fig. 7. (A) The SPR sensogram corresponding to the analyses of 1×10^{-7} to 1×10^{-3} M solutions of (a) NADPH, (b) NADH, (c) NAD^+, and (d) $NADP^+$, by the conducted using NADPH-imprinted polymeric films. Run (e) corresponds to the reanalysis of NAD(P)H. The numbers correspond to the respective analyte concentrations. (B) Calibration plots corresponding to the changes in the minimum reflectivity angles at variable concentrations of the $NAD(P)^+$/NAD(P)H cofactors: (a) for NADPH, (b) for NADH, (c) for $NADP^+$ and (d) for NAD^+.

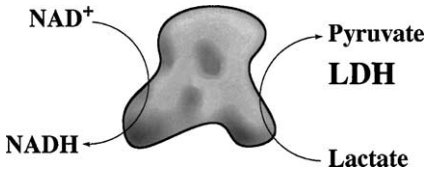

Fig. 8. Biocatalytic oxidation of lactate to pyruvate in the presence of NAD^+ and lactate dehydrogenase (LDH).

the other cofactors. These results clearly indicate that the NADH- and NADPH-imprinted polymers exhibit selectivity towards NADH and NADPH, respectively. Also, for the NADH and NADPH imprinted films we observe cyclic sensing activities, under continuous operation, for at least 2 days, with no observable degradation of the SPR signals. It should be noted that the $NADP^+$ or NADPH imprinted polymers do not only reveal selectivity towards the structurally related cofactor, but show also selectivity towards the bindings of other substrates that bind the boronic acid ligand. We find that the $NADP^+$ or NADPH imprinted polymers associated with the Au surface do not show any changes in the minimum reflectivity angle of the SPR spectra upon reaction with β-glucose or D(+)-galactose that bind to free boronic acid ligands. This suggests that the boronic acid ligands on the imprinted polymers are not accessible to these molecular substrates.

The NADH-imprinted film was then utilized to follow a biocatalytic process that involves the oxidation of lactate to pyruvate by NAD^+ in the presence of lactate dehydrogenase, LDH, Fig. 8. The NADH being formed in the biocatalytic process binds to the NADH-imprinted film and results in its swelling by the uptake of water. As before, the swelling leads to the increase of the polymer mass and an expected increase in the minimum reflectivity angle. The uptake of water, however, decreases the refractive index of the polymer, and concomitantly a decrease in the minimum reflectivity angle is observed. The experimental results indicate that the binding of NADH to the polymer film and the respective swelling has a higher influence of the refractive index on the resulting SPR spectrum, as reflected by the decrease of the minimum reflectivity angle.

Fig. 9 shows the sensogram that describes the analysis of the LDH-mediated oxidation of lactate. The NADH-imprinted polymer was assembled on the Au-coated glass support, and it was examined towards the sensing of variable concentrations of NADH, Fig. 9, run (a). Upon interaction with 1×10^{-3} M NADH, the minimum reflectivity angle of the functional polymer changes by $\Delta\theta_{min} = 8.2$ min. The polymer-bound NADH was washed off as evident by the regeneration of the reflectivity angle characteristic of the unloaded NADH-imprinted film (Fig. 9, point (*x*)). At point (*y*) the analysis of the biocatalyzed oxidation of lactate was initiated, run (b). At this point the oxidized cofactor, NAD^+, and the enzyme LDH were added to the system. A minute change in the minimum reflectivity angle that corresponds to the response of the NADH-imprinted film to NAD^+, is observed. At point (*z*) of run (b) after the signal stabilization, lactate, 1×10^{-2} M, was added to the system. The time-dependent changes in the minimum reflectivity angles of the polymer were observed (Fig. 9), inset, consistent with the biocatalyzed formation of NADH in the system and its sensing by the functional polymer. A control experiment reveals that addition of lactic acid alone to the system has no effect on the minimum reflectivity angle of

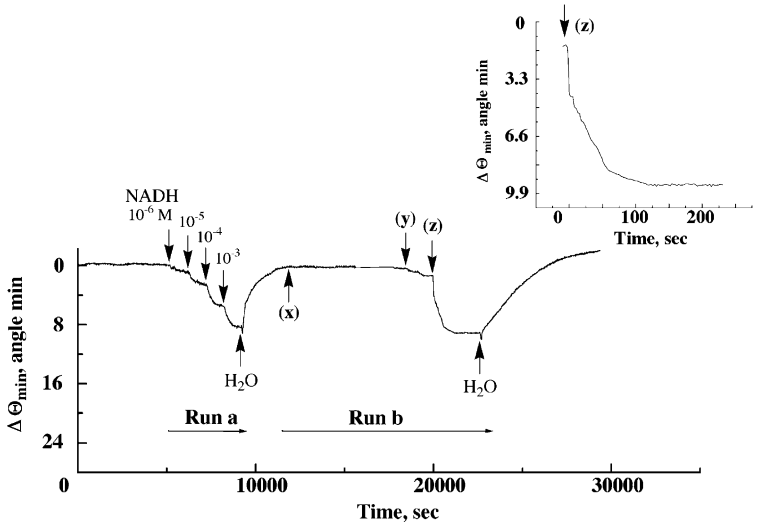

Fig. 9. The SPR sensogram corresponding to Run a the analysis of NADH, and Run b analysis of the LDH-mediated oxidation of lactate in the presence of NAD^+, using the NADH-imprinted polymer film as sensing interface. At point (*x*) the embedded NADH was washed off from the imprinted acrylamide-acrylamidophenylboronic acid copolymer. At point (*y*) NAD^+ (1×10^{-2} M) and the enzyme lactate dehydrogenase, 1×10^{-7} g ml^{-1} were injected into the phosphate buffer solution. After the signal stabilization (point (*z*)), lactic acid (1×10^{-2} M) was added to the system. The numbers correspond to the respective analyte concentrations. Inset shows enlarged time-dependent SPR response of the sensing interface in the presence of lactic acid (1×10^{-2} M), lactate dehydrogenase (1×10^{-7} g ml^{-1}), and NAD^+ (1×10^{-2} M).

the polymer. This implies that the observed changes in the minimum reflectivity angles originate from the biocatalyzed generation of NADH. The minimum reflectivity angle of the polymer film stabilizes at a value of $\Delta\theta_{min} = 7.9$ min, that is characteristic to the detection of ca. 1×10^{-3} M of NADH by the NADH-imprinted polymer (cf. Fig. 6(B)). This result is consistent with the fact that the concentration of NAD^+ in the system is 1×10^{-3} M, whereas the concentration of lactate is 10-fold higher, 1×10^{-2} M. Thus, the oxidized cofactor NAD^+ is essentially fully transformed to the reduced cofactor NADH, that is being sensed by the functional polymer. From the time-dependent changes in the minimum reflectivity angles (Fig. 9, inset) we calculate the pseudo first order rate constant $k = 3.2 \times 10^{-3}\ s^{-1}$ for the LDH biocatalyzed reduction of NAD^+ by lactate.

4. Conclusions

The present study has demonstrated the specific imprinting of recognition sites for the NAD^+, $NADP^+$, NADH and NADPH cofactors in an acrylamide-acrylamidophenylboronic acid copolymer film and the utilization of SPR spectroscopy as a means to follow the association of the different cofactors to the imprinted polymer films. We find that the association of the cofactors to the imprinted polymers results in the swelling of the polymer gel, a process that is followed by surface plasmon resonance spectroscopy. The use of SPR as a label-free optical detection means for the association of substrates to imprinted sites should be emphasized. So far, the use of SPR spectroscopy to follow binding processes in imprinted polymers is rare. The present study has also demonstrated the sensitivity of the method to identify the selective binding of the structurally related cofactors to the respective imprinted polymers.

We have also demonstrated the use of the NADH-imprinted film and SPR to follow the kinetics of the NAD^+-dependent lactate dehydrogenase biocatalyzed oxidation of lactate. This opens new possibilities to characterize $NAD(P)^+$ and NAD(P)H biocatalyzed reactions by optical detection means. Previous attempts based on the sensing of direct binding of low molecular-weight binding to the imprinted polymers demonstrated low signals and unsatisfactory analytical performance. The use of SPR as an optical readout signal for the association of substrates to imprinted sites provides a promising method with improved analytical characteristics.

Acknowledgements

This study is supported by the Israel Ministry of Science in the framework of Infrastructure Project on New Functional Materials.

References

[1] P.N. Bartlett, P. Tebbutt, R.G. Whitaker, Prog. React. Kinet. 16 (1991) 55.
[2] A.E. Biade, C. Bourdillon, J.M. Laval, G. Mairesse, J. Moiroux, J. Am. Chem. Soc. 114 (1992) 893.
[3] J.N. Burnett, A.L. Underwood, Biochemistry 4 (1965) 2060.
[4] A.J. Cunningham, A.L. Underwood, Biochemistry 6 (1967) 266.
[5] S. Chardonnoblat, S. Cosnier, A. Deronzier, N. Vlachopoulos, J. Electroanal. Chem. 352 (1993) 213.
[6] A. Bergel, M. Comtat, Bioelectrochem. Bioenerg. 27 (1992) 495.
[7] Y.-T. Long, H.-Y. Chen, J. Electroanal. Chem. 440 (1997) 239.
[8] W.J. Blaedel, R.A. Jenkins, Anal. Chem. 47 (1975) 1337.
[9] I. Katakis, E. Dominguez, Mikrochim. Acta 126 (1997) 11.
[10] L.L. Miller, J.R. Valentine, J. Am. Chem. Soc. 110 (1988) 3982.
[11] L. Gorton, J. Chem. Soc., Faraday Trans. 182 (1986) 1245.
[12] K. Haupt, K. Mosbach, Chem. Rev. 100 (2000) 2495.
[13] M. Zayats, M. Lahav, A.B. Kharitonov, I. Willner, Tetrahedron 58 (2002) 815.
[14] S.-W. Lee, I. Ichinose, T. Kunitake, Langmuir 14 (1998) 2857.
[15] B. Sellergren, K.J. Shea, J. Chromatogr. A 690 (1995) 29.
[16] G. Wulff, T. Gross, R. Schönfeld, Angew. Chem. Int. Ed. 36 (1997) 1962.
[17] B.R. Hart, K.J. Shea, J. Am. Chem. Soc. 123 (2001) 2072.
[18] M.J. Whitcombe, M.E. Rodriguez, P. Villar, E.N. Vulfson, J. Am. Chem. Soc. 117 (1995) 7105.
[19] L. Schweitz, L.I. Andersson, S. Nilsson, Anal. Chem. 69 (1997) 1179.
[20] P.T. Vallano, V.T. Remcho, J. Chromatogr. A 887 (2000) 125.
[21] M. Lahav, A.B. Kharitonov, I. Willner, Chem. Eur. J. 7 (2001) 3992.
[22] R. Makote, M.M. Collinson, Chem. Mater. 10 (1998) 2440.
[23] L. Schweitz, P. Spégel, S. Nilsson, Analyst 125 (2000) 1899.
[24] N.M. Brunkan, M.R. Gagne, J. Am. Chem. Soc. 122 (2000) 6217.
[25] W. Wang, S.H. Gao, B.H. Wang, Org. Lett. 1 (1999) 1209.
[26] I. Ichinose, T. Kikuchi, S.-W. Lee, T. Kunitake, Chem. Lett. (2002) 104.
[27] T.D. James, K.R.A.S. Sandanayake, S. Shinkai, Nature 374 (1995) 345.
[28] T.D. James, K. Murata, T. Harada, K. Ueda, S. Shinkai, Chem. Lett. (1994) 273.
[29] R. Gabai, N. Sallacan, V. Chegel, T. Bourenko, E. Katz, I. Willner, J. Phys. Chem. B 105 (2001) 8196.
[30] N. Sallacan, M. Zayats, T. Bourenko, A.B. Kharitonov, I. Willner, Anal. Chem. 74 (2002) 702.
[31] G. Wulff, J. Gimpel, Macromol. Chem. 183 (1982) 2469.
[32] G. Wulff, J. Haarer, Macromol. Chem. 192 (1991) 1329.
[33] W. Knoll, Annu. Rev. Phys. Chem. 49 (1998) 569.
[34] O.A. Raitman, E. Katz, A.F. Bückmann, I. Willner, J. Am. Chem. Soc. 124 (2002) 6487.
[35] Y. Iwasaki, T. Horiuchi, O. Niwa, Anal. Chem. 73 (2001) 1595.
[36] E. Kaganer, R. Pogreb, D. Davidov, I. Willner, Langmuir 15 (1999) 3920.
[37] A.J. Thiel, A.G. Frutos, C.E. Jordan, R.M. Corn, L.M. Smith, Anal. Chem. 69 (1997) 4948.
[38] W.A. Clark, X.Y. Jian, L. Chen, J.K. Northup, Biochem. J. 358 (2001) 389.
[39] A. Kugimiya, T. Takeuchi, Biosens. Bioelectron. 16 (2001) 1059.
[40] E.P.C. Lai, A. Fafara, V.A. van der Noot, M. Kono, B. Polsky, Can. J. Chem. 76 (1998) 265.
[41] S. Nishimura, T. Yoshidome, M. Higo, Anal. Sci. 17 (2001) i1697.
[42] S. Kitano, Y. Koyama, K. Kataoka, T. Okano, Y. Sakurai, J. Controll. Release 19 (1992) 162.
[43] G.V. Beketov, Y.M. Shirshov, O.V. Shynkarenko, V.I. Chegel, Sens. Actuators B 48 (1998) 432.